

Supramolecular Assembly of Tetramethylcucurbit[6]uril and 2-Picolylamine

Ying Fan,^{||} Ran Cen,^{||} Peihui Shan, Carl Redshaw, Hang Cong, Xin Xiao,* and Qingmei Ge*Cite This: *ACS Omega* 2023, 8, 9919–9924

Read Online

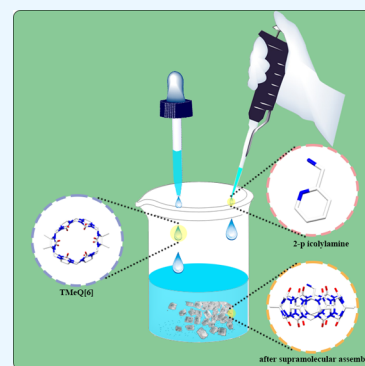
ACCESS |

Metrics & More

Article Recommendations

Supporting Information

ABSTRACT: The supramolecular assembly of symmetrical tetramethylcucurbit[6]uril (TMeQ[6]) and 2-picolylamine (AMPy) has been investigated via various techniques, including ultraviolet–visible (UV–vis) and nuclear magnetic resonance spectroscopy, isothermal titration calorimetry (ITC), and X-ray crystallography. The results indicated that TMeQ[6] could encapsulate the AMPy guest molecule to form a stable inclusion complex. The rotational restriction of the guest in the cavity of TMeQ[6] resulted in a large negative value of entropy. The X-ray crystal structure of the 1:1 inclusion complex between TMeQ[6] and AMPy revealed that AMPy exists in the elliptical cavity of TMeQ[6].



INTRODUCTION

Cucurbit[*n*]urils (Q[*n*], *n* = 5–8, 10, 13–15) consist of building blocks used for the construction of supramolecular switches, which can act as hosts in aqueous media for various static and stimuli-responsive guests.^{1–6} Recently, the functionalization of cucurbit[*n*]urils based on supramolecular catalysis^{7,8} and molecular recognition^{9,10} has received great attention. In 2004, the first alkyl-substituted symmetric tetramethylcucurbit[6]uril (TMeQ[6]) was discovered in our laboratory.¹¹ Compared with Q[6], TMeQ[6] features good water solubility and is often used to replace Q[6] in the study of host–guest chemistry^{12–18} and coordination chemistry.^{19,20}

2-Picolylamine (AMPy) is a bidentate amine used as a vital precursor for synthesizing various ionic liquids through the formation of β -amino alcohols as intermediates.²¹ It can also be used to functionalize poly(styrene-co-maleic anhydride) resin for facilitating the adsorption of uranium from an aqueous solution.²² In addition, AMPy is slightly hazardous to water and harmful to human health and the environment. Therefore, the capture of AMPy has become a vital environmental topic.

The supramolecular recognition of AMPy by cucurbit[*n*]urils has not been reported. Therefore, in this study, we reported a supramolecular assembly based on the complex of AMPy and $\alpha, \alpha', \delta, \delta'$ -tetramethylcucurbit[6]uril (TMeQ[6]) complexes. Scheme 1 depicts the structures of AMPy and TMeQ[6].

RESULTS AND DISCUSSION

Interaction of AMPy with TMeQ[6]. The electronic absorption spectrum of AMPy exhibited one absorption band

at 259 nm. With increasing TMeQ[6] concentrations, the intensity of the band was depressed. At a 1:1 molar ratio of TMeQ[6] to AMPy, the ultraviolet (UV) absorption intensity reached equilibrium (Figure 1a). Similar reduction of guest molar absorbance coefficients has been previously observed with other absorbing guests bounded to cucurbituril hosts. Figure 1b shows a plot of the absorbance band (at 259 nm) as a function of the added TMeQ[6] concentrations. The decreasing absorbance values of AMPy became equal after the addition of 1.0 equiv of TMeQ[6], indicating the formation of an AMPy (1:1) complex.

According to the linear Benesi–Hildebrand expression,²³ the measured absorbance [$1/(A - A_0)$] at 259 nm showed a linear relationship with a change in $1/[TMeQ[6]]$ ($R^2 = 0.9990$), indicating the 1:1 stoichiometry between TMeQ[6] and AMPy (Figure S1). To further confirm the stoichiometry of the complex, we recorded the corresponding Job plot, which exhibits a well-defined maximum at a molar fraction of guest equal to 0.5 (Figure 2), providing unequivocal evidence for the 1:1 stoichiometry of the supramolecular complex. According to the 1:1 stoichiometry and UV–vis titration data (Figure 2), the association constant of AMPy with TMeQ[6] in water was $(1.71 \pm 0.72) \times 10^4$ L/mol.

Received: November 2, 2022

Accepted: February 23, 2023

Published: March 6, 2023



Scheme 1. Structures of AMPy and TMeQ[6]

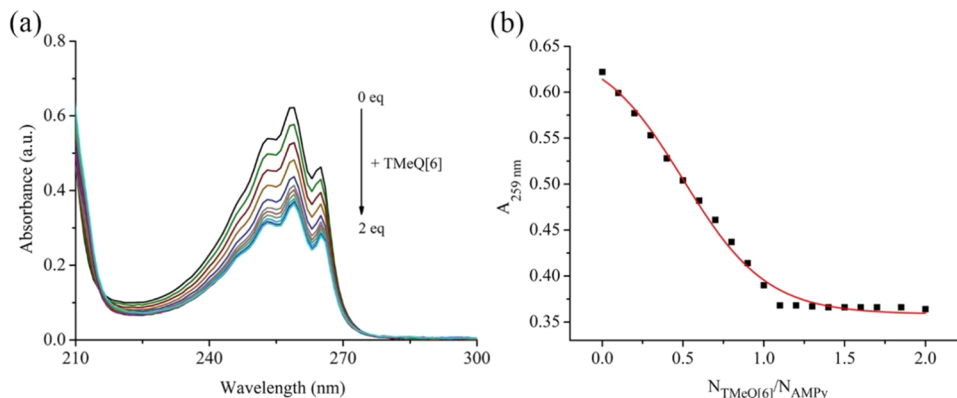
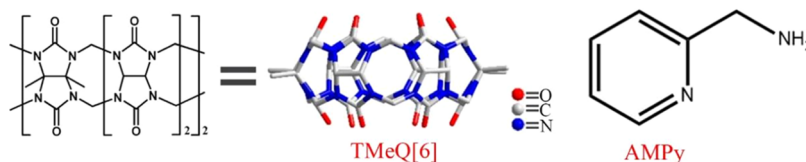


Figure 1. Interaction of AMPy and TMeQ[6]: (a) absorption spectra of AMPy (0.1 mM) in an aqueous solution containing different concentrations of TMeQ[6] and (b) the plot of concentration and absorbance vs $N_{\text{TMeQ[6]}}/N_{\text{AMPy}}$.

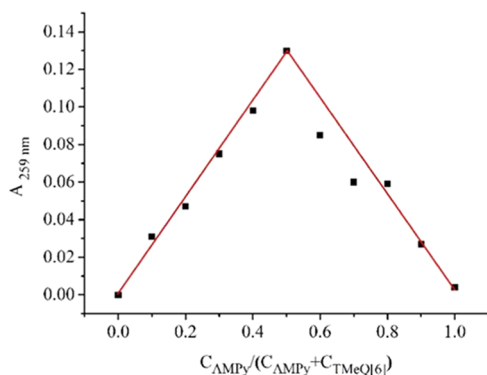


Figure 2. Job plot of guest AMPy with TMeQ[6].

Proton Nuclear Magnetic Resonance (^1H NMR) Spectroscopic Titrations of TMeQ[6] and AMPy. The complexation between TMeQ[6] and AMPy was studied via ^1H NMR spectroscopy. ^1H NMR titration experiments in D_2O provide direct evidence for a host–guest inclusion complex formation between AMPy and TMeQ[6]. Compared with the ^1H NMR spectrum of the unbound AMPy, the chemical shifts of the protons ($\Delta\delta$: $H_a = 0.55$ ppm, $H_b = 1.17$ ppm, $H_c = 1.36$ ppm, $H_d = 1.48$ ppm, and $H_e = 1.02$ ppm) in AMPy exhibited an upfield shift, indicating that AMPy exists in the cavity of TMeQ[6] (Figure 3).

Isothermal Titration Calorimetry (ITC). ITC experiments were performed to evaluate the binding models between AMPy and TMeQ[6], and the stoichiometry for the AMPy and TMeQ[6] complex was confirmed to be 1:1 with an association constant K_a of $5.373 \times 10^6 \text{ M}^{-1}$ (Figure 4). The results revealed that the complexation between AMPy and TMeQ[6] is driven by enthalpy and entropy ($\Delta H = -51.29 \text{ kJ mol}^{-1}$, $\Delta S = -43.19 \text{ kJ mol}^{-1}$, and $\Delta G = -38.42 \text{ kJ mol}^{-1}$) (Table 1). The ITC data showed that the host–guest complexation was advantageous in both enthalpy and entropy. The K_a value indicated an effective combination between

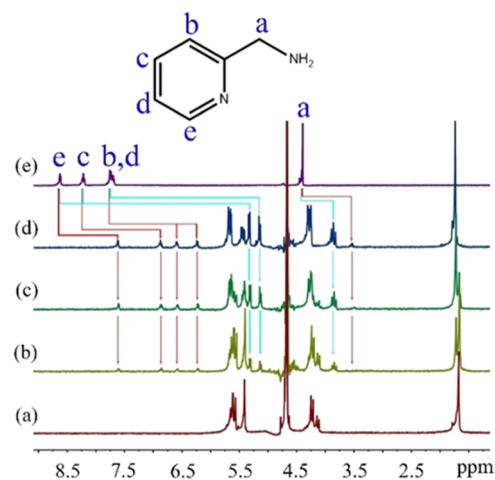


Figure 3. Titration ^1H NMR spectra (400 MHz, D_2O) of TMeQ[6] in the presence of (a) 0.00, (b) 1.00, (c) 2.00, (d) 3.00 equiv of AMPy, and (e) AMPy.

AMPy and TMeQ[6]. The negative enthalpy change ($\Delta H = -53.96 \text{ kJ mol}^{-1}$) and negative entropy change ($\Delta S = -43.19 \text{ kJ mol}^{-1}$) indicated that the formation of AMPy and TMeQ[6] inclusion compounds was driven by favorable enthalpy changes, followed by a smaller negative (unfavorable) entropy change.

Single-Crystal X-ray Diffraction. The binding behavior between TMeQ[6] and the AMPy guest molecule in a solid state was investigated via X-ray diffraction. Numerous attempts were made to form suitable crystalline samples, and in this study, we presented a crystal structure of the host–guest complex, namely, $[(\text{C}_{40}\text{H}_{54}\text{N}_{24}\text{O}_{17})@(\text{Sr} \cdot (\text{C}_6\text{H}_9\text{N}_2) \cdot 2(\text{NO}_3) \cdot 5(\text{H}_2\text{O}))]$. The single-crystal X-ray diffraction analysis revealed that the complex was crystallized in the monoclinic crystal system with a $P2_1/c$ space group. The asymmetric unit of the complex contained one TMeQ[6] host, one AMPy molecule, one strontium ion, and both bound and unbound water

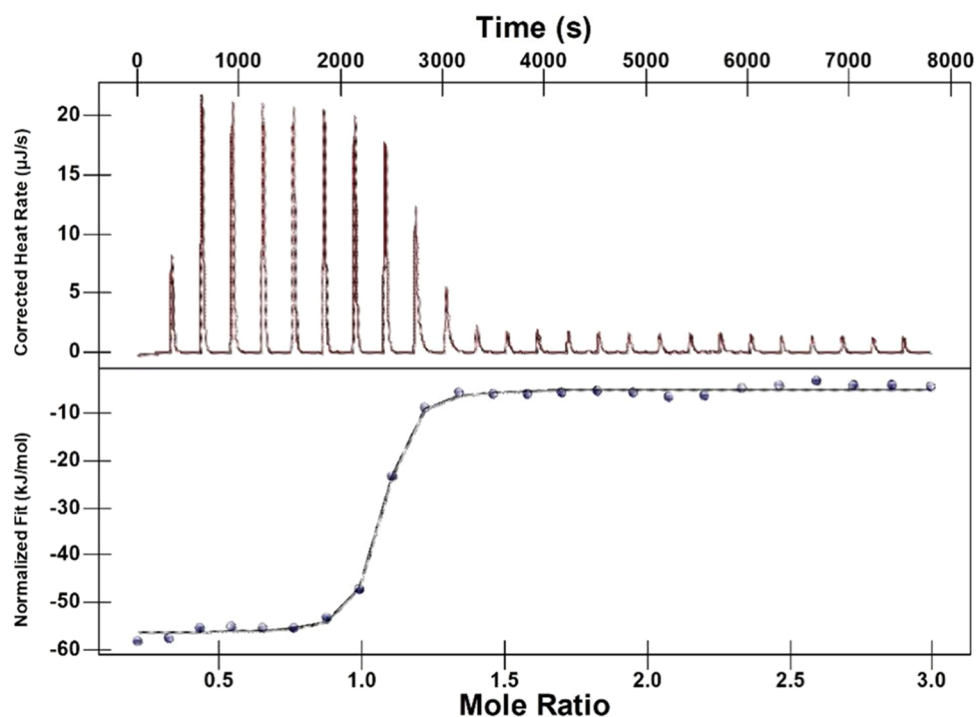


Figure 4. ITC profile of host TMeQ[6] with guest AMPy at 298.15 K.

Table 1. Thermodynamic Parameters of AMPy/TMeQ[6]

K_a (M^{-1})	ΔH ($kJ\ mol^{-1}$)	ΔG ($kJ\ mol^{-1}$)	ΔS ($kJ\ mol^{-1}$)	n
5.37×10^6	-51.29 ± 0.006	-38.42	-43.19	$1.016 \pm 4.15 \times 10^{-5}$

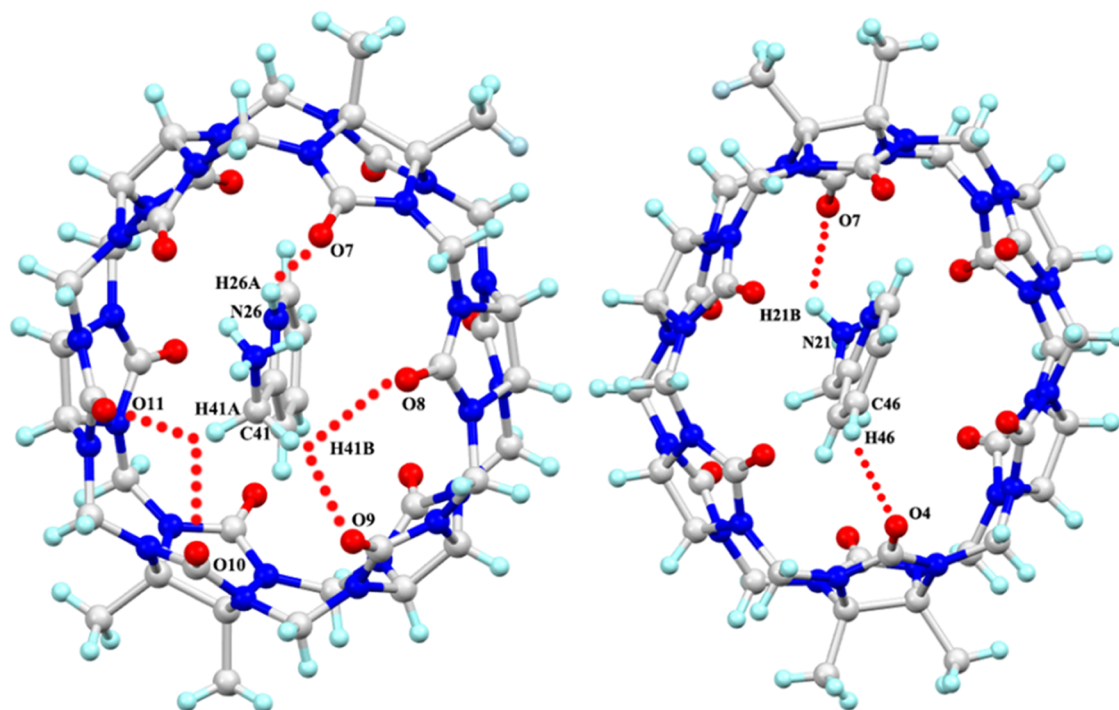


Figure 5. Ball-and-stick representation of compound showing guest molecule encapsulated into the TMeQ[6] host, generating an inclusion complex. Water molecules and strontium ion are omitted for clarity (C = light gray, O = red, N = blue, and H = light blue).

molecules. The AMPy guest molecule was encapsulated in the cavity of the TMeQ[6] host except for the amino group, consistent with the results in an aqueous solution via 1H NMR spectroscopy (Figure 5).

The encapsulated AMPy formed numerous hydrogen bonds with the TMeQ[6] host, in which the ammonium group of AMPy pointed toward one carbonyl oxygen atom of TMeQ[6] (Figure 5). The hydrogen bonding between one proton of the

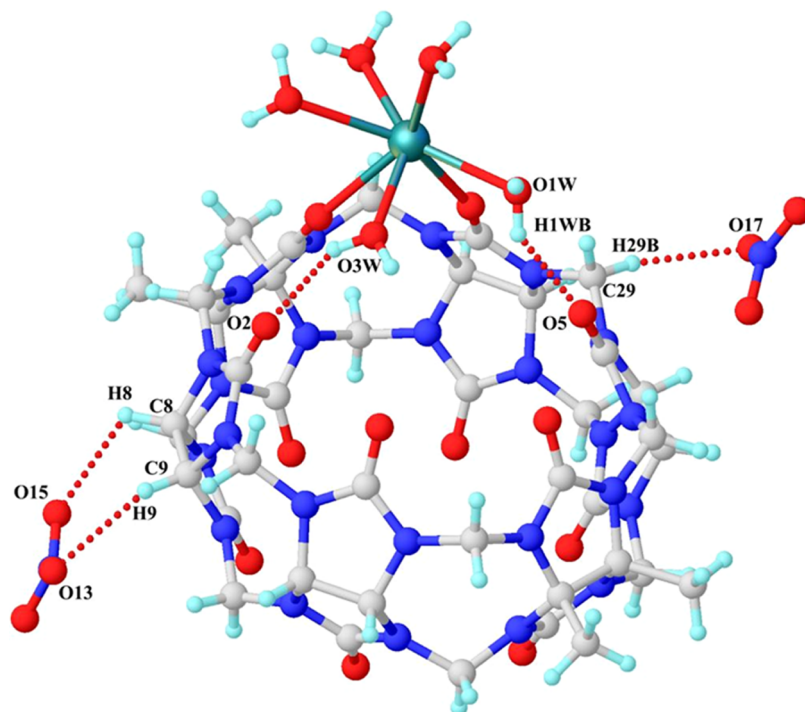


Figure 6. X-ray crystal structure of the inclusion complex. Unbound water molecules and guest molecule are omitted.

ammonium group and one carbonyl oxygen atom featured an N(26)–H(26A)⋯O(7) distance at 2.563 Å. The hydrogen-bonding interactions between the carbon atoms of methylene and the portal carbonyl oxygen atoms of TMeQ[6] exhibited distances for C(41)–H(41B)⋯O(8) at 2.764 Å, C(41)–H(41B)⋯O(9) at 2.464 Å, C(41)–H(41A)⋯O(10) at 2.679 Å, and C(41)–H(41A)⋯O(11) at 2.395 Å. The hydrogen-bonding interactions between the carbon atoms of the pyridyl and the portal carbonyl oxygen atoms of TMeQ[6] exhibited distances for N(21)–H(21B)⋯O(7) at 2.247 Å, and C(46)–H(46)⋯O(4) at 2.847 Å.

Each strontium ion was coordinated with five water molecules and two carbonyl oxygen atoms of TMeQ[6] (Figure 6). The hydrogen-bonding interactions between the oxygen atoms of the bound water molecules and the portal carbonyl oxygen atoms of TMeQ[6] exhibited distances for O(1W)–H(1WB)⋯O(5) at 2.069 Å, and O(3W)–H(3WA)⋯O(2) at 2.038 Å. Moreover, abundant hydrogen bonding occurred between the nitrate ions and the hydrogen atoms of TMeQ[6]. The hydrogen-bonding interactions between the oxygen atoms of the nitrate ions and the hydrogen atoms of TMeQ[6] featured distances for C(8)–H(8)⋯O(15) at 2.467 Å, and C(9)–H(9)⋯O(13) at 2.447 Å, and C(29)–H(29B)⋯O(17) at 2.486 Å. The abundant hydrogen-bonding interactions contributed to the formation of stable inclusion complexes.

CONCLUSIONS

We have investigated the host–guest complexation between TMeQ[6] and AMPy via UV–vis and ¹H NMR spectroscopy and ITC in a solution. The results showed that almost all AMPy guest molecules were encapsulated in the cavity of TMeQ[6]. Furthermore, a crystal structure of the complex provided direct evidence for the host–guest inclusion complex, with hydrophobic and hydrogen-bonding interactions in the solid state. The hydrophobic forces facilitated by the cavity of

TMeQ[6] acted upon the pyridine rings of AMPy. The hydrogen-bonding interactions between the oxygen atoms of TMeQ[6] and amino group, and methylene and the portal carbonyl oxygen atoms of TMeQ[6], were both consistent in the solid state of the solution.

EXPERIMENTAL SECTION

Materials. TMeQ[6] was synthesized in our laboratory,²⁴ and AMPy was purchased from Aladdin (Shanghai, China). All reagents are of analytical reagent grade and can be used without further purification. Deionized water was used throughout.

Instruments. UV-2700 spectrum. Nano ITC Isothermal Titration Calorimeter (TA, America). All NMR data were recorded on a Bruker DPX 400 spectrometer in D₂O at 293.15 K.

¹H NMR Spectroscopic Measurements. The ¹H NMR spectra were recorded on a JEOL jmm-ecz400s spectrometer at 25 °C. D₂O was used as a field frequency lock, and the observed chemical shifts are reported in parts per million (ppm) relative to the built-in tetramethylsilane (TMS) standard (0.0 ppm).

Isothermal Titration Calorimetry. TMeQ[6] is made into 2.00 × 10^{−4} mol/L stock solutions, and AMPy is made into 1.00 × 10^{−2} mol/L stock solution for later use. AMPy (5.00 × 10^{−5} mol/L) was titrated with TMeQ[6] (2.00 × 10^{−4} mol/L); stirring speed was 250 r/min, sample cell volume was 1300 μL 250 s/drop, 8 μL/drop. The titration temperature was 25 °C, and water was used as the reference.

Single-Crystal X-ray Crystallography. TMeQ[6] (15.00 mg, 0.012 mmol) and SrCl₂ (10.00 mg, 0.063 mmol) were added to AMPy (6.60 mg, 0.061 mmol) in dilute HNO₃ solution (3 mL). The mixture was stirred for 3 min at 70 °C and was filtered. The filtrate slowly evaporated (about 3 weeks) in air, and block colorless crystals of the complex were obtained.

Single-crystal data for the complex were collected using the Bruker Smart Apex II CCD diffractometer with graphite-monochromated Mo K α radiation ($\lambda = 0.71073$ Å) at 293(2) K. An empirical absorption correction was applied using the SADABS program.²⁵ All complex structures were solved with SHELXT, completed through subsequent difference Fourier syntheses, and refined on F2 using SHELXL-201820 (full-matrix least-squares techniques) in the Olex2 package. All nonhydrogen atoms in the whole structure were refined with anisotropic displacement parameters. Carbon-bound hydrogen atoms were introduced at calculated positions and were treated as riding atoms with an isotropic displacement parameter equal to 1.2 times that of the parent atom. The platon-SQUEEZE routine was used for all compounds owing to the disordered solvent water molecules. CCDC 2213570 contains the supporting crystallographic data for this study. These data can be obtained freely from the Cambridge Crystallographic Data Centre via www.ccdc.cam.ac.uk/data_request/cif.

■ ASSOCIATED CONTENT

SI Supporting Information

The Supporting Information is available free of charge at <https://pubs.acs.org/doi/10.1021/acsomega.2c06989>.

Materials and instruments; preparation of crystals; crystal data; and calculation of association constant (PDF)

■ AUTHOR INFORMATION

Corresponding Authors

Xin Xiao – Key Laboratory of Macrocyclic and Supramolecular Chemistry of Guizhou Province, Guizhou University, Institute of Applied Chemistry, Guizhou University, Guiyang 550025, China; orcid.org/0000-0001-6432-2875; Email: gyhxxiao@163.com, xxiao@gzu.edu.cn

Qingmei Ge – Key Laboratory of Macrocyclic and Supramolecular Chemistry of Guizhou Province, Guizhou University, Institute of Applied Chemistry, Guizhou University, Guiyang 550025, China; Enterprise Technology Center of Guizhou Province, Guizhou University, Guiyang 550025, China; orcid.org/0000-0002-4918-4176; Email: qmge@gzu.edu.cn

Authors

Ying Fan – Key Laboratory of Macrocyclic and Supramolecular Chemistry of Guizhou Province, Guizhou University, Institute of Applied Chemistry, Guizhou University, Guiyang 550025, China

Ran Cen – Key Laboratory of Macrocyclic and Supramolecular Chemistry of Guizhou Province, Guizhou University, Institute of Applied Chemistry, Guizhou University, Guiyang 550025, China

Peihui Shan – Key Laboratory of Macrocyclic and Supramolecular Chemistry of Guizhou Province, Guizhou University, Institute of Applied Chemistry, Guizhou University, Guiyang 550025, China

Carl Redshaw – Department of Chemistry, University of Hull, Hull HU6 7RX, U.K.; orcid.org/0000-0002-2090-1688

Hang Cong – Key Laboratory of Macrocyclic and Supramolecular Chemistry of Guizhou Province, Guizhou University, Institute of Applied Chemistry, Guizhou University, Guiyang 550025, China; Enterprise Technology

Center of Guizhou Province, Guizhou University, Guiyang 550025, China; orcid.org/0000-0001-6855-5123

Complete contact information is available at: <https://pubs.acs.org/doi/10.1021/acsomega.2c06989>

Author Contributions

Y.F. and R.C. have contributed equally as first authors. All authors had full access to all of the data in the study and take responsibility for the integrity of the data and the accuracy of the data analysis.

Notes

The authors declare no competing financial interest.

■ ACKNOWLEDGMENTS

This work was supported by the Natural Science Foundation of Guizhou Province (no. [2020]1Y028), Research Project of Introduce Talents of Guizhou University (no. (2019)02), and National Natural Science Foundation of China (no. 22002027).

■ REFERENCES

- (1) (a) Lee, J. W.; Samal, S.; Selvapalam, N.; Kim, H. J.; Kim, K. Cucurbituril Homologues and Derivatives: New Opportunities in Supramolecular Chemistry. *Acc. Chem. Res.* **2003**, *36*, 621–630. (b) Lagona, J.; Mukhopadhyay, P.; Chakrabarti, S.; Isaacs, L. The cucurbit[n]uril family. *Angew. Chem., Int. Ed.* **2005**, *44*, 4844–4870. (c) Isaacs, L. Cucurbit[n]urils: from mechanism to structure and function. *Chem. Commun.* **2009**, 619–629. (d) Masson, E.; Ling, X.; Joseph, R.; Kyeremeh-Mensah, L.; Lu, X. Cucurbituril chemistry: a tale of supramolecular success. *RSC Adv.* **2012**, *2*, 1213–1247. (e) Barrow, S. J.; Kasera, S.; Rowland, M. J.; del Barrio, J.; Scherman, O. A. Cucurbituril-based molecular recognition. *Chem. Rev.* **2015**, *115*, 12320–12406.
- (2) Liu, M.; Chen, L. X.; Shan, P. H.; Lian, C. J.; Zhang, Z. H.; Zhang, Y. Q.; Tao, Z.; Xiao, X. Pyridine detection using supramolecular organic frameworks incorporating cucurbit[10]uril. *ACS Appl. Mater. Interfaces* **2021**, *13*, 7434–7442.
- (3) Liu, M.; Cen, R.; Li, J. S.; Li, Q.; Tao, Z.; Xiao, X.; Isaacs, L. Double-cavity nor-seco-cucurbit[10]uril enables efficient and rapid separation of pyridine from mixtures of toluene, benzene, and pyridine. *Angew. Chem., Int. Ed.* **2022**, *61*, No. e202207209.
- (4) Yang, D.; Liu, M.; Xiao, X.; Tao, Z.; Redshaw, C. Polymeric self-assembled cucurbit[n]urils: Synthesis, structures and applications. *Coord. Chem. Rev.* **2021**, *434*, No. 213733.
- (5) Liu, M.; Kan, J. L.; Yao, Y. Q.; Zhang, Y. Q.; Bian, B.; Tao, Z.; Zhu, Q. J.; Xiao, X. Facile preparation and application of luminescent cucurbit[10]uril-based porous supramolecular frameworks. *Sens. Actuators, B* **2019**, *283*, 290–297.
- (6) Gao, R. H.; Chen, L. X.; Chen, K.; Tao, Z.; Xiao, X. Development of hydroxylated cucurbit[n]urils, their derivatives and potential applications. *Coord. Chem. Rev.* **2017**, *348*, 1–24.
- (7) Assaf, K. I.; Nau, W. M. Cucurbiturils: from synthesis to high-affinity binding and catalysis. *Chem. Soc. Rev.* **2015**, *44*, 394–418.
- (8) Cong, H.; Chen, Q.; Geng, Q.; Tao, Z.; Yamato, T. IBX oxidation of benzenedimethanols in the presence of cucurbit[8]uril. *Chin. J. Chem.* **2015**, *33*, 545–549.
- (9) Elbashir, A. A.; Aboul-Enein, H. Y. Supramolecular analytical application of cucurbit[n]urils using fluorescence spectroscopy. *Crit. Rev. Anal. Chem.* **2015**, *45*, 52–61.
- (10) Barrow, S. J.; Kasera, S.; Rowland, M. J.; del Barrio, J.; Scherman, O. A. Cucurbituril-based molecular recognition. *Chem. Rev.* **2015**, *115*, 12320–12406.
- (11) Zhao, Y. J.; Xue, S. F.; Zhu, Q. J.; Tao, Z.; Zhang, J. X.; Wei, Z. B.; Long, L. S.; Hu, M. L.; Xiao, H. P.; Day, A. Synthesis of a symmetrical tetrasubstituted cucurbit[6]uril and its host-guest

inclusion complex with 2,2'-bipyridine. *Chin. Sci. Bull.* **2004**, *49*, 1111–1116.

(12) Cong, H.; Tao, L. L.; Yu, Y. H.; Tao, Z.; Yang, F.; Zhao, Y. J.; Xue, S. F.; Lawrence, G. A.; Wei, G. Interaction between tetramethylcucurbit[6]uril and some pyridine derivatives. *J. Phys. Chem. A* **2007**, *111*, 2715–2721.

(13) Zeng, J. P.; Zhang, S. M.; Zhang, Y. Q.; Tao, Z.; Zhu, Q. J.; Xue, S. F.; Wei, G. Use of silver(I) and copper(II) ions to assist the self-assembly of polyrotaxanes incorporating symmetrical $\alpha, \alpha', \delta, \delta'$ -tetramethyl-cucurbit[6]uril. *Cryst. Growth Des.* **2010**, *10*, 4509–4515.

(14) Yang, B.; Zheng, L. M.; Gao, Z. Z.; Xiao, X.; Zhu, Q. J.; Xue, S. F.; Tao, Z.; Liu, J. X.; Wei, G. Extended and contorted conformations of alkanediammonium ions in symmetrical $\alpha, \alpha', \delta, \delta'$ -tetramethylcucurbit[6]uril Cavity. *J. Org. Chem.* **2014**, *79*, 11194–11198.

(15) Xiao, X.; Gao, Z. Z.; Shan, C. L.; Tao, Z.; Zhu, Q. J.; Xue, S. F.; Liu, J. X. Encapsulation of haloalkane 1-(3-chlorophenyl)-4-(3-chloropropyl)-piperazinium in symmetrical $\alpha, \alpha', \delta, \delta'$ -tetramethylcucurbit[6]uril. *Phys. Chem.* **2015**, *17*, 8618–8621.

(16) Huang, Y. H.; Geng, Q. X.; Jin, X. Y.; Cong, H.; Qiu, F.; Xu, L.; Tao, Z.; Wei, G. Tetramethylcucurbit[6]uril-triggered fluorescence emission and its application for recognition of rare earth cations. *Sens. Actuators, B* **2017**, *243*, 1102–1108.

(17) Saha, S.; Dutta, B.; Ghosh, M.; Chowdhury, J. Adsorption of 4-Mercapto Pyridine with Gold Nanoparticles Embedded in the Langmuir-Blodgett Film Matrix of Stearic Acid: SERS, XPS Studies Aided by Born-Oppenheimer on the Fly Dynamics, Time-Resolved Wavelet Transform Theory, and DFT. *ACS Omega* **2022**, *7*, 27818–27830.

(18) Lin, Q.; Guan, X. W.; Zhang, Y. M.; Wang, J.; Fan, Y. Q.; Yao, H.; Wei, T. B. Spongy Materials Based on Supramolecular Polymer Networks for Detection and Separation of Broad-Spectrum Pollutants. *ACS Sustainable Chem. Eng.* **2019**, *7*, 14775–14784.

(19) Chen, W. J.; Yu, D. H.; Xiao, X.; Zhang, Y. Q.; Zhu, Q. J.; Xue, S. F.; Tao, Z.; Wei, G. Difference of coordination between alkali- and alkaline-earth-metal ions to a symmetrical $\alpha, \alpha', \delta, \delta'$ -tetramethylcucurbit[6]uril. *Inorg. Chem.* **2011**, *50*, 6956–6964.

(20) Yang, B.; Gao, Z. Z.; Lu, J. H.; Zhu, Q. J.; Xue, S. F.; Tao, Z.; Prior, T. J.; Redshaw, C.; Wei, G.; Xiao, X. Interaction of a symmetrical $\alpha, \alpha', \delta, \delta'$ -tetramethyl-cucurbit[6]uril with Ln^{3+} : potential applications for isolation of lanthanides. *CrystEngComm* **2016**, *18*, 5028–5035.

(21) Fringuelli, F.; Pizzo, F.; Tortoioli, S.; Vaccaro, L. Solvent-free $\text{Al}(\text{OTf})_3$ -catalyzed aminolysis of 1,2-epoxides by 2-picolylamine: A key step in the synthesis of ionic liquids. *J. Org. Chem.* **2004**, *69*, 7745–7747.

(22) Liu, S. D.; Yang, Y.; Liu, T. H.; Wu, W. S. Recovery of uranium(VI) from aqueous solution by 2-picolylamine functionalized poly(styrene-co-maleic anhydride) resin. *J. Colloid Interface Sci.* **2017**, *497*, 385–392.

(23) Thordarson, P. Determining association constants from titration experiments in supramolecular chemistry. *Chem. Soc. Rev.* **2011**, *40*, 1305–1323.

(24) Zhao, Y. J.; Xue, S. F.; Zhu, Q. J.; Tao, Z.; Zhang, J. X.; Wei, Z. B.; Long, L. S.; Hu, M. L.; Xiao, H. P.; Day, A. I. Synthesis of a symmetrical tetrasubstituted cucurbit[6]uril and its host-guest inclusion complex with 2,2'-bipyridine. *Chin. Sci. Bull.* **2004**, *49*, 1111–1116.

(25) Dolomanov, O. V.; Bourhis, L. J.; Gildea, R. J.; Howard, J. A. K.; Puschmann, H. OLEX2: a complete structure solution, refinement and analysis program. *J. Appl. Cryst.* **2009**, *42*, 339–341.